THE JOURNAL OF BIOLOGICAL CHEMISTRY
Vol. 277, No. 39, Issue of September 27, pp. 36415–36424, 2002

Printed in U.S.A.

Calpain Activity Regulates the Cell Surface Distribution of Amyloid Precursor Protein

INHIBITION OF CALPAINS ENHANCES ENDOSOMAL GENERATION OF β-CLEAVED C-TERMINAL APP FRAGMENTS*

Received for publication, May 28, 2002
Published, JBC Papers in Press, June 26, 2002, DOI 10.1074/jbc.M205208200

Paul M. Mathews‡§¶, Ying Jiang‡, Stephen D. Schmidt‡, Olivera M. Grbovic‡, Marc Mercken‖, and Ralph A. Nixon‡§

From the ‡Nathan Kline Institute and §New York University School of Medicine, Orangeburg, New York 10962 and ‖Johnson and Johnson Pharmaceutical Research and Development, Janssen Pharmaceutica, Turnhoutseweg 30, B-2340 Beerse, Belgium

In murine L cells, treatment with calpeptin or calpain inhibitor III increased Aβ42, but not Aβ40, secretion in a dose-dependent fashion. This correlated with an increase in the levels of amyloid precursor protein (APP) carboxyl-terminal fragments (CTFs). Immunoprecipitation with novel mAbs directed against the carboxyl-terminus of APP or specific for the β-cleaved CTF showed that generation of both α- and β-cleaved CTFs increase proportionately following inhibition of calpains. Pulse-chase metabolic labeling confirmed that inhibiting calpains increases the production of α- and β-cleaved APP metabolites. Immunolabeling showed greater βCTF signal in calpeptin-treated cells, primarily in small vesicular compartments that were shown to be predominantly endosomal by colocalization with early endosomal antigen 1. A second mAb, which recognizes an extracellular/luminal epitope found on both APP and βCTFs, gave more cell surface labeling of calpeptin-treated cells than control cells. Quantitative binding of this antibody confirmed that inhibiting calpains caused a partial redistribution of APP to the cell surface. These results demonstrate that 1) calpain inhibition results in a partial redistribution of APP to the cell surface, 2) this redistribution leads to an increase in both α- and β-cleavage without changing the ratio of αCTFs/βCTFs, and 3) the bulk of the βCTFs in the cell are within early endosomes, confirming the importance of this compartment in APP processing.

The deposition of the small (~40–42 residues) Aβ peptide as insoluble β-amyloid plaque in the brain parenchyma is an invariant feature of Alzheimer's disease. Aβ is generated by proteolysis of the ~100-kDa amyloid precursor protein (APP),[1] a broadly expressed type 1 transmembrane protein that is found primarily in the trans-Golgi network (TGN) and at the cell surface (reviewed in Ref. 1). The β-cleavage of APP occurs within the luminal/extracellular domain of APP and generates two APP fragments: a large, soluble amino-terminal fragment (sAPPβ) that is secreted from the cell and a transmembrane, carboxyl-terminal fragment (CTF) that remains associated with the cell. This βCTF consists of 99 amino acids, contains the whole Aβ peptide, and has a molecular mass of ~10 kDa. An alternative pathway involves the cleavage of APP 16 residues downstream of this site at the α-cleavage site. Like β-cleavage, α-cleavage generates a sAPP fragment (sAPPα) that is secreted from the cell and an αCTF (of 84 residues and ~8 kDa) that remains membrane-associated. α-Cleavage occurs within the Aβ peptide sequence and as such prevents the generation of Aβ from a given APP molecule. Aβ is generated from the βCTF by an intramembrane cleavage (γ-cleavage) that occurs primarily at 40 residues, and to a lesser extent 42 residues, downstream from the β-cleavage site, releasing Aβ1–40 or Aβ1–42.

Much progress has been made recently in identifying the major proteases/protease complexes responsible for α-, β-, and γ-cleavage (the α-, β-, and γ-secretases). α-Cleavage appears to be due to the activity of two metalloproteases (TACE and ADAM10) and is thought to occur primarily at the cell surface (2–7). The BACE proteases, a recently identified family of transmembrane apartyl proteases, appear to account for much of the β-secretase activity within normal cells (8, 9). BACE has an endosomal-lysosomal pattern of distribution as well as an acidic pH optimum (9–11); BACE-mediated cleavage of APP in the endocytic system is consistent with prior work that has identified, through various trafficking mutants of APP, the early endosome as an important site for Aβ generation (12–14) and as a compartment showing functional alterations at the earliest stages of AD (15). The presenilin (PS) proteins play an intimate role in γ-cleavage; expression of familial AD-causing mutant presenilin increases the production of Aβ terminating at residue 42 (16–18), the PS-null phenotype includes the inability of the cell to generate Aβ and the intracellular accumulation of CTFs (19, 20), and recent work has directly implicated PS itself as the γ-secretase (21), although other proteins within the PS complex such as nicastrin (22) may well be directly involved in γ-cleavage.

The calpain system consists of two Ca^{2+}-activated, cytosolic, neutral pH, cysteine proteases, which are typically distinguished by their different affinities for Ca^{2+} *in vitro* (m-calpain and μ-calpain), as well as an endogenous inhibitor, calpastatin (23–25). Calpains play a central role in cytoskeleton remodel-

* This work was supported by the National Institute of Aging, the Alzheimer's Association, and the New York State Office for Mental Hygiene. The costs of publication of this article were defrayed in part by the payment of page charges. This article must therefore be hereby marked "*advertisement*" in accordance with 18 U.S.C. Section 1734 solely to indicate this fact.

¶ To whom correspondence should be addressed: Nathan Kline Institute and New York University School of Medicine, 140 Old Orangeburg Rd., Orangeburg, NY 10962. Tel.: 845-398-5428; Fax: 845-398-5422; E-mail: mathews@nki.rfmh.org.

[1] The abbreviations used are: APP, amyloid precursor protein; sAPP, soluble amino-terminal APP fragment; CTF, carboxyl-terminal fragment; TGN, trans-Golgi network; PS, presenilin; AD, Alzheimer's disease; ELISA, enzyme-linked immunosorbent assay; EEA1, early endosomal antigen 1; mAb, monoclonal antibody.

TABLE I
Monoclonal antibodies

The monoclonal antibodies used in this study are listed, as well as the known epitope specificities based upon the antigen used for immunization and the antibody's binding by ELISA to synthetic peptides. The binding of these antibodies to various APP proteolytic species is as characterized in this study and in similar results (P.M. Mathews and Y. Jiang), unpublished results). The species specificity for each antibody has been determined empirically.

Name	Epitope specificity	APP species detected	Species specificity
C1/6.1	Carboxyl-terminal 20 residues of APP	APP holoprotein, all CTFs	Mouse/human
JRF/AβN/25	First 7 residues of Aβ; requires β-cleavage	βCTF, Aβ1-X by ELISA	Mouse/human
JRF/Aβtot/17	Within residues 1–16 of human Aβ	APP holoprotein, βCTF, Aβ by ELISA	Human
JRF/rAβ1–15/2	Within residues 1–15 of mouse Aβ	Aβ by ELISA	Mouse
JRF/cAβ40/10	Carboxyl terminus of Aβ40	Aβ40 by ELISA	Mouse/human
JRF/cAβ42/26	Carboxyl terminus of Aβ42	Aβ42 by ELISA	Mouse/human

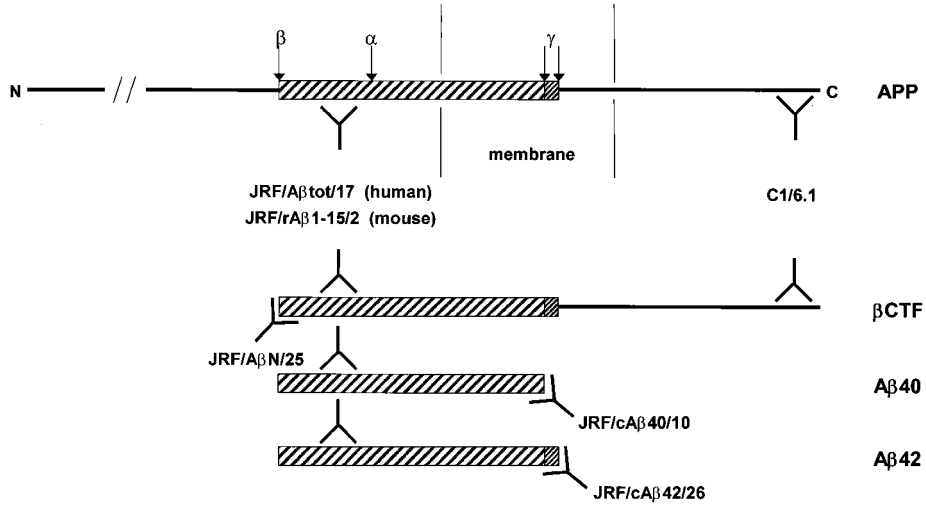

FIG. 1. **Schematic diagram showing monoclonal antibody binding to APP and APP metabolites.** The Aβ domain is *hatched*, showing alternative γ40- or 42-cleavage. Binding specificities for the monoclonal antibodies described in Table I are illustrated.

ing (26), have been suggested to play a regulatory role in some vesicular transport events (27), and are the primary mediators of cell death following an unregulated increase in intracellular Ca^{2+} concentration, as occurs with excitotoxicity (28, 29). The calpain system appears to be up-regulated during AD, with evidence that both m-calpain and μ-calpain are abnormally activated in neurons (30–32). These changes in the calpain system are most often thought to impact tau metabolism, due in part to their known roles in tau turnover (33, 34) and regulation of kinases thought to be involved in tau hyperphosphorylation and proteolysis (32, 33, 35).

Calpain activity may also modulate Aβ production. Inhibiting calpain activity increases Aβ production by cells in culture, with Aβ42 increasing more than Aβ40 (36–39). In addition, calpain inhibitors have been shown to increase the levels of CTFs in cells (39, 40). Zhang *et al.* (39) examined this effect in cells overexpressing an APP βCTF construct and concluded that the increase in CTFs was due to their stabilization, but the mechanism(s) underlying such an increase in CTFs derived from APP holoprotein has yet to be examined in detail.

To this end, we have examined the metabolism and intracellular distribution of APP in cells following treatment with calpain inhibitors. Our results confirm that calpain inhibitors greatly increase Aβ42 generation, while having a smaller effect on Aβ40. We found that inhibiting calpains resulted in a substantial and proportionate increase in the generation of both α- and β-cleaved CTFs and that this increase in the production of CTFs is likely to be the result of a partial redistribution of APP from the TGN to the plasma membrane. Using a monoclonal antibody that specifically recognizes the βCTF, we show that βCTFs colocalize with a marker of the early endosome, both without treatment and following calpain inhibitor treatment. These data suggest a model in which inhibiting the calpain system drives a greater proportion of APP to the cell surface and early endosomes, where α-cleavage and β-cleavage, respectively, can then occur. The additional βCTFs generated are then substrate for γ-42-secretase activity, further linking the generation of this highly pathogenic species of Aβ to the early endosome.

MATERIALS AND METHODS

Cell Lines, cDNA Constructs, and Transfections—Ltk cells (a murine fibroblast-like cell line (41)) were maintained at 37 °C and 5% CO_2 in high glucose Dulbecco's modified Eagle's medium (Cellgro, Herndon, VA) supplemented with 10% fetal bovine serum (Invitrogen), 2 mM glutamax I (Invitrogen), and penicillin/streptomycin (Cellgro). cDNAs encoding human APP_{695} (42) or PS1 with the P117L mutation (43) were inserted into the mammalian expression vector pcDNA3 (Invitrogen). Following transfection using Lipofectin (manufacturer's protocol; Invitrogen), stable L cell lines were selected in 400 μg/ml G418 (Invitrogen) and screened for expression (42, 44). N2a (17) and IMR-32 (45) neuroblastomas were obtained from the American Type Culture Collection (Gaithersburg, MD) and maintained as recommended by the ATCC.

Antibodies—Table I describes the six monoclonal antibodies directed against APP and/or APP metabolites used in this study; Fig. 1 is a schematic diagram showing the use of these antibodies to detect APP metabolites. C1/6.1 was raised against the conserved carboxyl-terminal 20 residues of APP (residues 676–695 of APP_{695}) and is useful for immunolabeling, immunoprecipitation, and Western blot analysis (42). JRF/AβN/25 was raised against a synthetic peptide encompassing residues 1–7 of human Aβ. Evidence that JRF/AβN/25 requires β-cleavage at residue 1 of Aβ has been presented by Vandermeeren *et al.* (46) and is substantiated by this study. JRF/Aβtot/17 was raised against human Aβ1–40; mapping of its epitope against synthetic peptides has demonstrated that JRF/Aβtot/17 binds within residues 1–15 and is specific for human Aβ. JRF/rAβ1–15/2 was raised against a synthetic peptide encompassing residues 1–15 of murine Aβ and does not recognize human Aβ or human APP (42, 46). JRF/cAβ40/10 was raised against the carboxyl-terminal 5 residues of Aβ1–40, and JRF/cAβ42/26 was raised against the carboxyl-terminal 10 residues of Aβ1–42. These Aβ carboxyl-terminal antibodies, their specificity, and their use in our sandwich ELISA has been recently described (42, 47). The anti-APP-luminal

domain monoclonal antibody P2–1 was the generous gift of Dr. Maria Kounnas SIBIA/Merck (La Jolla, CA) (48); monoclonal antibody 6E10 was purchased from Senetek. Purified anti-early endosomal antigen 1 (EEA1) rabbit serum was the kind gift of Dr. S. Corvera (Department of Cell Biology, University of Massachusetts Medical School, Worcester, MA) (49, 50).

Sandwich ELISAs—Sandwich ELISAs using these antibodies were done essentially as previously reported (42, 47, 51), with modifications to detect either human or murine Aβ secreted into the growth media. Nunc-Immuno Plates (Nunc A/S, Roskilde, Denmark) were coated overnight at 4 °C using a 10 μg/ml concentration of either JRF/cAβ40/10 in 10 mM Tris, 10 mM NaCl, pH 8.5, or JRF/cAβ42/26 in 100 mM bicarbonate buffer, pH 9.6, and the remaining protein binding sites were blocked by incubating with 1% Block Ace (Dainippon Pharmaceutical, Osaka, Japan) in PBS for 4 h at room temperature. Cells were seeded onto six-well dishes and allowed to settle overnight. Human APP or $PS1_{P117L}$ expression in L cells was induced with 20 mM butyrate for ~40 h (41), whereas neuroblastoma lines were allowed to grow to near confluence. Growth medium was then replaced with 0.8 ml of fresh medium containing calpeptin or calpain inhibitor III (Calbiochem) and, for transfected L cells, butyrate. After 6 h, this conditioned medium was collected and HEPES (pH 7.4) was added to 25 mM and loaded undiluted into duplicate wells for ELISA. Human and murine Aβ1–40 and Aβ1–42 peptide standards were purchased from American Peptide Co. (Sunnyvale, CA); stock solutions were stored at −70 °C and further diluted immediately prior to use. ELISA plates were incubated overnight at 4 °C with samples and standards. Aβ was detected by incubating for 4 h at room temperature with horseradish peroxidase-conjugated JRF/Aβtot/17 (human Aβ) or JRF/rAβ1–15/2 (murine Aβ) diluted in 20 mM sodium phosphate, 2 mM EDTA, 400 mM NaCl, 1% bovine serum albumin, pH 7.0. ELISA plates were developed using a color reaction (TMB Microwell Peroxidase Substrate System, Kirkegaard & Perry, Gaithersburg, MD), and the A_{450} was read. ELISA signals are reported as the mean ± S.E. of two or more wells in fmol of Aβ/ml of medium.

Metabolic Labeling, Immunoprecipitation, and Western Blot Analysis—To detect APP and CTFs, 5×10^5 cells were seeded onto 35-mm diameter tissue culture dishes followed by induction with 20 mM butyrate for 24 h (41). Cultures were methionine/cysteine-starved for 20 min, pulse-labeled for 15 min with 100 μCi/ml Tran^{35}S-label (PerkinElmer Life Sciences), washed, and chased in complete medium containing 2 mM unlabeled methionine (41). Calpain inhibitors, as described under "Results," were added to the growth media 3 h prior to methionine/cysteine starvation and then throughout pulse labeling and chase. Cell lysates (prepared in 1% Triton X-100, 140 mM NaC1, 25 mM Tris, pH 7.4, 0.5 mM EDTA, 10 mM methionine, and protease inhibitors (41, 52)) were subjected to immunoprecipitation with one of several monoclonal antibodies as described under "Results." Sequential immunoprecipitation of the growth medium to isolate metabolically labeled sAPPα and sAPPβ has been described (42). Immunoprecipitated proteins were sized by SDS-PAGE, and labeled proteins visualized by exposure to x-ray film and analyzed quantitatively using a Storm 840 PhosphorImager (Amersham Biosciences) and/or by scan analysis (NIH Image).

For Western blot analysis, protein concentration in cell lysates was determined (Bio-Rad DC Protein Assay), and equal amounts of proteins were separated by SDS-PAGE gels and transferred to polyvinylidene difluoride membrane. Membranes were incubated in C1/6.1 (2 μg/ml) overnight, washed, and incubated with horseradish peroxidase-conjugated goat anti-mouse IgG for 1.5 h. Membranes were washed, and ECL substrate (Amersham Biosciences) was added before exposure to x-ray film.

Quantitative ^{125}I-mAb Binding—Sodium [^{125}I]iodide was purchased from PerkinElmer Life Sciences. Monoclonal antibodies JRF/Aβtot/17 and JRF/AβN/25 were iodinated using iodogen tubes (Pierce; manufacturer's protocol), and ^{125}I-mAb was recovered (41). APP-overexpressing L cells grown in six-well dishes were butyrate-induced for ~40 h as described above, fixed at room temperature (as for immunolabeling) and incubated for 2 h with 10^6 cpm ^{125}I-mAb (adjusted to 2 μg/ml total mAb with unlabeled mAb) in Hanks' balanced salt solution, 10% horse serum, 20 mM HEPES (pH 7.4) as previously described (41). Following washes, bound ^{125}I-mAb was recovered in 2 ml of 1 N NaOH and counted in a γ counter. 0.1% saponin (w/v; Sigma) was added to the binding solution to permeabilize cells. Nonspecific binding was estimated using identical cultures of nontransfected L cells and a 50-fold excess of unlabeled mAb in the binding solution; all data points represent nonspecific binding subtracted from specific binding, each the mean of triplicate measurements ± S.E.

Immunolabeling—For indirect immunofluorescence labeling, L cells were seeded onto glass coverslips, and expression of APP was induced. Cells were fixed in 4% paraformaldehyde, 5% sucrose in PBS (pH 7.4) at room temperature for 15 min and immunolabeled as previously described (41). Fluorescein- and Texas Red-coupled secondary antibodies were purchased from Cappel (Durham, NC). Cells were permeabilized by the addition of 0.1% saponin to the antibody-containing solutions. Cells were mounted in Vectashield (Vector Laboratories, Burlingame, CA) and examined by epifluorescence and laser confocal microscopy.

TABLE II

Treatment with calpeptin preferentially increases Aβ42 production

The growth medium for the indicated cells was replaced with control medium or medium containing 10 μM calpeptin, and the Aβ secreted in 6 h was measured by sandwich ELISA as described under "Materials and Methods."

Cell line	Percentage of control ± S.E. following 10 μM calpeptin treatment
L cell	%
Murine Aβ40	116 ± 3
Murine Aβ42	200 ± 11
$L/PS1_{P117L}$	
Murine Aβ40	135 ± 1
Murine Aβ42	281 ± 19
L/APP	
Human Aβ40	103 ± 2
Human Aβ42	339 ± 37
N2a	
Murine Aβ40	110 ± 8
Murine Aβ42	278 ± 17
IMR-32	
Human Aβ40	106 ± 2
Human Aβ42	289 ± 46

RESULTS

Calpain Inhibitors Increase Aβ42 Secretion Selectively While Increasing CTF Levels—Initially, we sought to confirm previous findings (36–38), which have showed that inhibition of calpains predominantly affected Aβ by increasing Aβ42 production, using a murine fibroblast-like line (L cells) as well as murine and human neuroblastoma lines (Table II). By sandwich ELISA, we determined the amount of Aβ40 and Aβ42 secreted into the growth media over a 6-h period by control cells or by cells treated with the calpain inhibitor calpeptin. In L cells, calpeptin treatment consistently increased the amount of secreted Aβ42, typically 2–3-fold over that secreted by control cells, while increasing Aβ40 secretion less than 1.5-fold. In an L cell line expressing an FAD mutant PS1 ($L/PS1_{P117L}$) (43), again we found that Aβ42 increased more than Aβ40, although the initial levels of Aβ42 were higher due to expression of the mutant PS1 (see Fig. 2). When we examined Aβ secretion in an L cell line expressing human APP_{695} (L/APP) (42) using an ELISA specific for human Aβ, we obtained similar results, with Aβ40 essentially unchanged and Aβ42 again increased 3.5-fold by calpeptin treatment. Similar increases with calpeptin treatment were also seen in the murine neuroblastoma cell line N2a and the human hippocampal neuroblastoma line IMR-32 (45), with Aβ42 increasing ~3-fold and Aβ40 remaining nearly unchanged. These data emphasize that calpain inhibition with calpeptin has a much greater effect on Aβ42 than on Aβ40 and, importantly, that this effect is seen in nonneuronal as well as neuron-like cells.

Previous reports have shown that, in addition to increasing Aβ42 production, inhibiting calpains increases the steady-state level of APP CTFs detected within cells (39, 40). In the experiment shown in Fig. 2, we examined the interrelationship between Aβ production and the steady-state CTF levels following calpain inhibition in L cells. Fig. 2*A* shows ELISA data for Aβ generated from the endogenous murine APP in L cells and in L cells expressing a mutant presenilin 1 ($PS1_{P117L}$) (43) at increasing concentrations of calpain inhibitor III. Aβ40 levels in the parental and the $PS1_{P117L}$-expressing L cells were found to

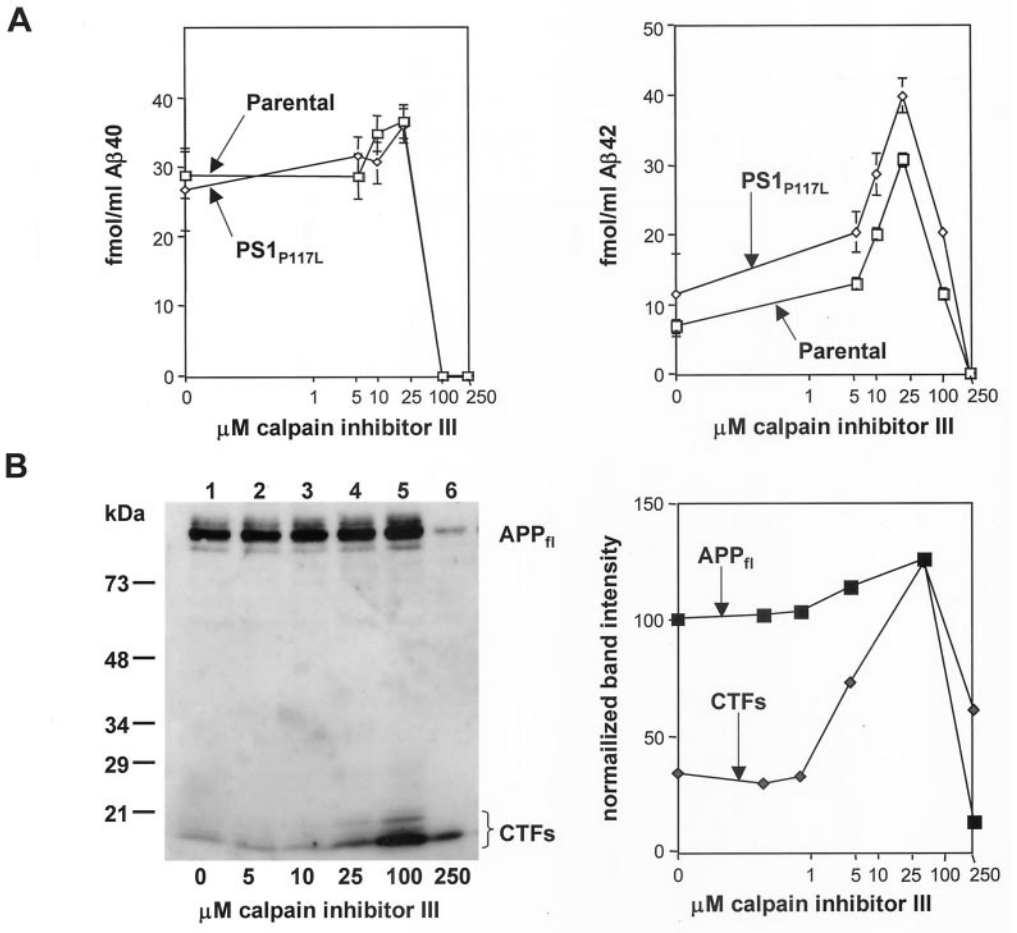

FIG. 2. **Calpain inhibitor III increases Aβ42 in a dose-dependent fashion while increasing the levels of APP CTFs.** L cells or L cells expressing a familial AD-causing presenilin 1 mutation ($PS1_{P117L}$) (43) were treated with the indicated concentration of calpain inhibitor III for 6 h. Conditioned media were collected and analyzed by sandwich ELISA for murine Aβ40 and Aβ42 (*A*). *B*, cell lysates were prepared, and proteins were sized by SDS-PAGE prior to Western blot analysis using C1/6.1; full-length APP (APP_{fl}) and CTFs are indicated in the Western blot and the quantitation of this blot. Similar results were obtained with calpeptin (data not shown).

be similar and did not increase significantly with calpain inhibitor III at any concentration. Base-line Aβ42 production was greater in the mutant PS1-expressing L cells. 5–25 μM calpain inhibitor III treatment resulted in a nearly parallel increase in Aβ42 produced by either the control or $PS1_{P117L}$-expressing L cells. Both Aβ40 and Aβ42 levels were found to dramatically decrease to below detectability at the highest calpain inhibitor III concentrations (100 and 250 μM). Additional experiments, including pulse-metabolic labeling and immunoprecipitation of APP, demonstrated that this was the result of calpain inhibitor III blocking protein biosynthesis at these high concentrations (data not shown). This is consistent with the observations of Zhang *et al.* (39) that high concentrations of calpain inhibitors decreased both Aβ40 and Aβ42 generation and may explain an apparent decrease in CTF degradation at these toxic concentrations.

We initially examined the relationship between CTF levels and calpain inhibition by Western blot analysis using the monoclonal antibody C1/6.1 (42), which was raised against the carboxyl-terminal 20 amino acids of APP and recognizes the holoprotein as well as multiple CTFs (Fig. 2*B*). Quantitation of this Western blot demonstrates a substantial increase in CTF levels with increasing calpain inhibitor III concentrations. At the highest concentration, however, both APP holoprotein, and to a lesser extent, CTFs decline precipitously, which is consistent with these high doses of the inhibitor blocking protein biosynthesis. These results demonstrate that CTF levels and Aβ42 production following calpain inhibition correlate strongly.

Calpain Inhibitors Increase the Generation Of Both α- and β-Cleaved APP Metabolites—To determine what species of CTFs were appearing following calpain inhibitor treatment, we immunoprecipitated APP holoprotein and CTFs using a set of monoclonal antibodies that recognize different epitopes within the carboxyl-terminal 99 residues of APP (see Table I). In addition to the monoclonal antibody C1/6.1, we used two monoclonal antibodies raised against Aβ epitopes: JRF/AβN/25, which was raised against a peptide consisting of the amino-terminal 7 residues of Aβ, and JRF/Aβtot/17, which was raised against Aβ1–40 and has been shown by peptide-epitope mapping to recognize a sequence contained within residues 1–16 of human Aβ. In the experiment shown in Fig. 3, L cells overexpressing human APP_{695} (L/APP cells) were metabolically labeled for 15 min followed by a chase for 1 h. Cells were treated for 3 h prior to as well as during the pulse and chase periods with the indicated calpain inhibitors. Equal volumes of detergent lysates prepared from the pulse and chase periods were subjected to immunoprecipitation with each monoclonal antibody, and labeled APP species were resolved by 4–20% gradient SDS-PAGE. In untreated L/APP cells (Fig. 3, *lanes 1–6*), C1/6.1 immunoprecipitated labeled holoprotein from the pulse period (*lane 1*). Following a 1-h chase, C1/6.1 immunoprecipitation also revealed two rapidly migrating APP fragments that migrated at ~10 and 8 kDa, consistent in size with the αCTF and βCTF (Fig. 3, lane 4; *arrows* indicating αCTF and βCTF). JRF/AβN/25 immunoprecipitation failed to bring down APP holoprotein (*lanes 2* and *5*), confirming peptide mapping data (not shown) indicating that the epitope for JRF/AβN/25 re-

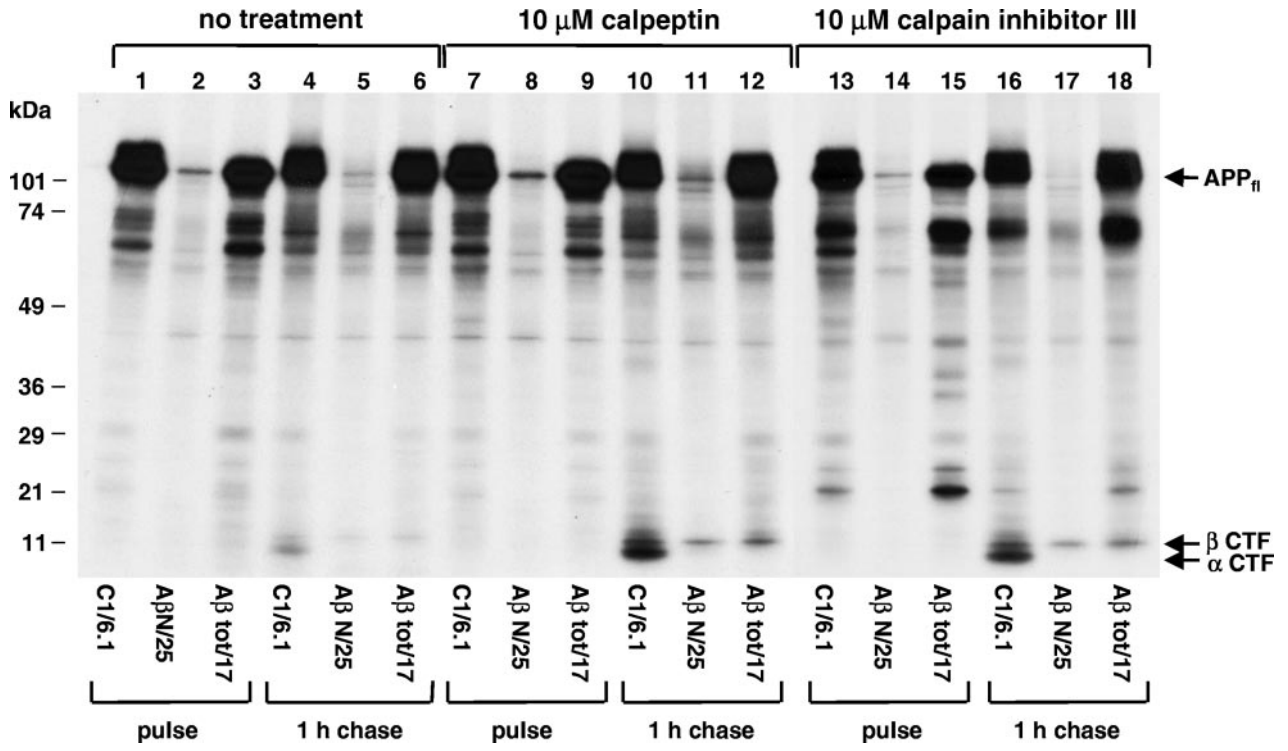

FIG. 3. **Calpain inhibitors increase the generation of both α- and β-cleaved CTFs.** An L cell line overexpressing human APP was metabolically labeled for 15 min and chased for 1 h as indicated. Cells were pretreated with the indicated calpain inhibitors for 3 h prior to metabolic labeling as well as during labeling and chase. Cell lysates were prepared, and equal volumes were immunoprecipitated with one of three monoclonal antibodies: C1/6.1, which recognizes an epitope within the 20 carboxyl-terminal-most residues of APP; JRF/AβN/25, which recognizes residues 1–7 of Aβ; and JRF/Aβtot/17, which recognizes an epitope within residues 1–16 of Aβ. Labeled, immunoprecipitated proteins were sized on SDS-PAGE and detected as described under "Materials and Methods." The *arrows* indicate the APP holoprotein (*APP$_{fl}$*) and the α- and β-cleaved CTFs (αCTF and βCTF, respectively).

quires a cleaved amino terminus at residue 1 of Aβ. That JRF/AβN/25 immunoprecipitated, following the 1-h chase, a protein that co-migrated with one of the CTFs revealed by C1/6.1 immunoprecipitation (compare *lanes 4* and *5*) conclusively identifies this as the β-cleaved CTF of APP. JRF/Aβtot/17 immunoprecipitated APP holoprotein in the pulse and chase periods (*lanes 3* and *6*, respectively), as well as the βCTF following chase. Given the specificities of these three monoclonal antibodies and the mobility on SDS-PAGE of the CTFs they immunoprecipitate, we conclude that the most rapidly migrating species identified by C1/6.1 is the α-cleaved CTF.

In cells treated with either 10 μM calpeptin or 10 μM calpain inhibitor III, the immunoprecipitation pattern from the pulse-labeled lysates was similar to that seen from untreated cells (compare *lanes 1–3* with *lanes 7–9* and *13–15*), although calpain inhibitor III treatment increased the relative signal from a number of bands detected by C1/6.1 and JRF/Aβtot/17 that migrated more rapidly than APP holoprotein but more slowly than the CTFs. With calpain inhibition, striking differences in the abundance of CTFs, however, were seen following a 1-h chase. C1/6.1 immunoprecipitation demonstrated a substantial and apparently proportionate increase in the levels of both αCTFs and βCTFs with either calpain inhibitor (*compare lane 4* with *lanes 10* and *16*). This increase in the βCTF was confirmed by immunoprecipitation with JRF/AβN/25 and JRF/Aβtot/17 (*lanes 11*, *12*, *17*, and *18*). Densitometric quantitation of these bands from the C1/6.1 immunoprecipitation confirmed our observation that the ratio of αCTF to βCTF appears not to be affected by calpain inhibition (remaining at ~2:1) despite an approximate 4-fold increase in both CTFs. Finally, it should be noted that the APP holoprotein contains 5 times more methionines than do the CTFs, so that metabolic labeling substantially underestimates the relative abundance of the CTFs.

The 1-h chase shown in Fig. 3 suggests that calpain inhibition increases the production of CTFs, although a slowing of their turnover might have the same effect. We directly addressed the generation and turnover of the CTFs as well as the production of sAPP in the pulse-chase experiment shown in Figs. 4 and 5. In Fig. 4, L/APP cells were pulse-labeled for 15 min and chased for the indicated times up to 6 h prior to immunoprecipitation of lysates with C1/6.1. In Fig. 4*A*, the *top panel* shows that the turnover of APP holoprotein in control (*lanes 1–6*) and 10 μM calpeptin-treated cells (*lanes 7–12*) is similar. The *bottom panel* shows a longer exposure of the same immunoprecipitation showing the generation and turnover of the CTFs. In agreement with the data in Fig. 3, 10 μM calpeptin treatment substantially increased the generation of both α and β CTFs during the initial 1 h of chase (compare *lanes 1–3* with *lanes 7–9*); in contrast to a previous interpretation (39), however, this calpeptin concentration did not appear to reduce the turnover of CTFs. Quantitation of these data confirmed that the turnover of APP holoprotein is unchanged by calpeptin treatment (Fig. 4*B*). Additionally, the rate of CTF degradation, like the turnover of APP, does not appear to be affected by calpeptin treatment. These findings also support the hypothesis that the increase in Aβ42 seen following calpain inhibition is due to increased production of βCTFs. Indeed, with calpeptin treatment and at 1-h chase, the combined αCTF and βCTF signal accounts for ~40% of the metabolically labeled APP present in the pulse period, indicating the importance of these metabolic pathways following calpain inhibition.

In order to demonstrate that calpain inhibition promotes the α- and β-cleavage of APP, we immunoprecipitated sAPPα and sAPPβ from the growth media of untreated L/APP cells (Fig. 5, *lanes 1–4*) and calpeptin-treated cells (*lanes 5–8*) at various chase times following a 15-min pulse labeling. In general,

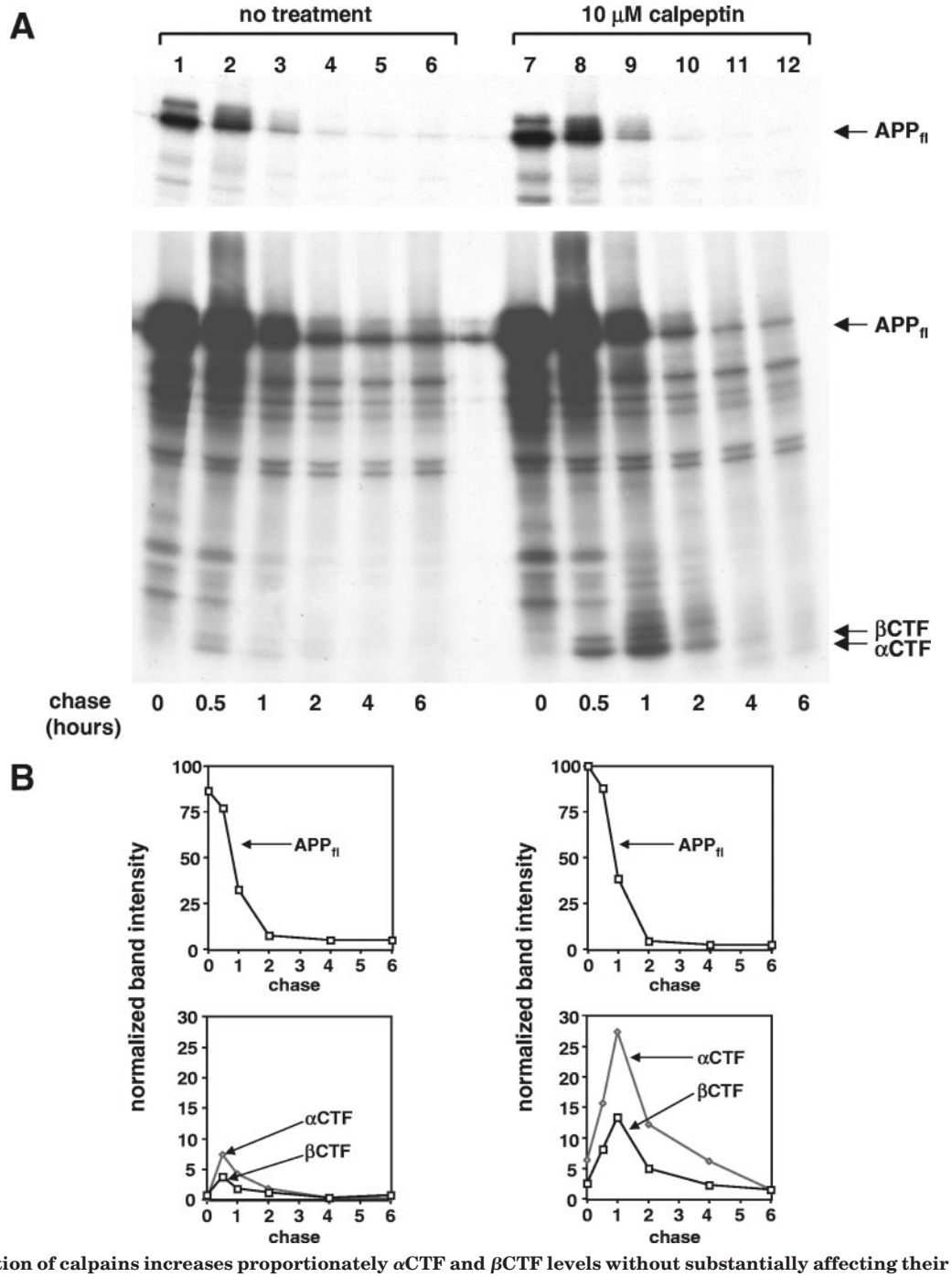

FIG. 4. **Inhibition of calpains increases proportionately αCTF and βCTF levels without substantially affecting their turnover rate.** The L cell line overexpressing APP was metabolically labeled and chased for the indicated times. Calpeptin treatment was performed as in Fig. 3. Cell lysates were immunoprecipitated with C1/6.1. The *top panel* in *A* is a short exposure showing the turnover of the APP holoprotein (APP_{fl}). The *bottom panel* is a longer exposure showing the APP holoprotein and the α- and β-cleaved CTFs (αCTF and βCTF). *B*, quantitation of this pulse-chase experiment is shown, illustrating the rapid turnover of the APP holoprotein, which is unaffected by calpeptin treatment, and the dramatic and proportionate increase in αCTF and βCTF generation with calpeptin treatment.

greater levels of sAPPα and sAPPβ were seen in the calpeptin-treated cells when compared with the control cells. In both conditions, sAPPα and sAPPβ were detectable after a 1-h chase, with their levels increasing significantly by 2 h of chase time. Whereas sAPP levels remained constant from 2–4-h chase time in the untreated cells, a small increase in both sAPPα and sAPPβ levels was seen in the calpeptin-treated cells between 2 and 3 h (compare *lanes 6* and *7*). Since sAPP levels were found to be nearly maximal after a 2-h chase period, we performed a series of four pulse-labeling experiments in which sAPPα and sAPPβ were immunoprecipitated following a 2-h chase period from untreated and 10 μM calpeptin-treated cells. Quantitation of these experiments showed a greater than 2-fold increase of both sAPPα and sAPPβ levels in the media of calpeptin-treated cells *versus* untreated cells (sAPPα, 2.2 ± 0.8; sAPPβ, 2.4 ± 0.6; mean increase of calpeptin-treated cells relative to untreated cells ± S.E.). Given that both sAPP species appear to be quite stable in the growth media in both control conditions as well as following calpain inhibition, the likely explanation for an increase in sAPPα and sAPPβ levels following calpeptin treatment is an increase in α- and β-cleavage of APP. This result argues that calpain inhibition results in an increase in these cleavage events and, therefore, an increase in the production of sAPPα, sAPPβ, αCTF, and βCTF. It should

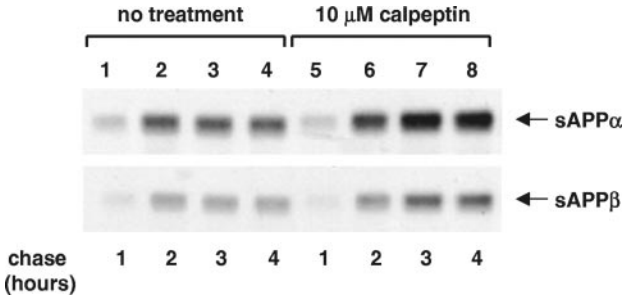

FIG. 5. **sAPPα and sAPPβ production increases following calpain inhibition.** L/APP cells were metabolically labeled for 15 min and chased for the indicated times. sAPPα and sAPPβ were isolated from the chase media by sequential immunoprecipitation using 6E10 to first capture sAPPα followed by P2-1 (48) immunoprecipitation to isolate the remaining sAPPβ (42). Cells were treated with 10 μM calpeptin as described in the legend to Fig. 3.

be noted, however, that the increase in maximal CTF levels detected by pulse-chase labeling was found to be greater (~4-fold; see Fig. 4) than the increase in sAPP levels shown above, suggesting that part of the calpain inhibitor effect may be a slowing in the turnover of the CTFs after their generation. While we cannot rule out this possibility, our pulse-chase data (Fig. 4) show that the stability of the CTFs following calpain inhibition is not extended greatly.

βCTFs Colocalize with an Early Endosomal Marker, EEA1—That JRF/AβN/25 specifically recognizes the βCTF of APP allowed us to determine the levels and intracellular distribution of this APP proteolytic fragment by immunolabeling. Fig. 6 shows the JRF/AβN/25 labeling pattern in control L/APP cells (*A–C*) and L/APP cells treated for 6 h with 10 μM calpeptin (*D–F*). JRF/AβN/25 primarily decorated small, punctate structures distributed throughout the cell (A). Consistent with our Western blot and metabolic labeling data, the intensity of JRF/AβN/25 immunolabeling increased following calpeptin treatment, although the pattern of labeling was similar (Fig. 6, compare *A* with *D*). Given that this pattern suggests a small vesicular compartment and previous work that has suggested early endosomes as a likely site of APP proteolysis leading to Aβ generation (12, 13, 15), we co-immunolabeled with a polyclonal antibody directed against early endosomal antigen 1 (Fig. 6, *B* and *E*), a protein that interacts with the early endosomal membrane and associated regulatory proteins (49, 50, 53, 54). JRF/AβN/25-labeled βCTFs showed striking coincidence with EEA1, both in the control cells (*C*) and the calpeptin-treated cells (*F*). This co-immunolabeling result suggests that many of the βCTF within these cells are located in early endocytic compartments and that calpain inhibition does not substantially alter this distribution.

Calpain Inhibitors Cause a Partial Redistribution of APP to the Cell Surface—We performed similar immunolabeling experiments using JRF/Aβtot/17, which recognizes APP holoprotein as well as the βCTF, and C1/6.1, which recognizes APP holoprotein and all CTFs. Fig. 7 shows co-immunolabeling with JRF/Aβtot/17 and the EEA1 antiserum; results with C1/6.1 were similar. In control L/APP cells, JRF/Aβtot/17 showed strong perinuclear labeling, consistent with an important TGN localization for APP, as well as lesser labeling of peripheral structures (*A*). With calpeptin treatment, however, JRF/Aβtot/17 showed similar perinuclear labeling yet much greater labeling of the cell's periphery (*E*). This peripheral labeling included demarcation of the cell's surface, which we confirmed to be plasma membrane localization by demonstrating immunolabeling of nonpermeabilized cells with JRF/Aβtot/17 (Fig. 7, compare *D* (untreated cells), with *H* (calpeptin-treated cells)). A consistent finding by immunolabeling was greater JRF/Aβtot/17 binding at the cell surface following calpain inhibition. The EEA1 localization (Fig. 7, *B* and *F*) and the overlay of JRF/Aβtot/17 and EEA1 immunolabeling in these cells (*C* and *G*), demonstrated that, unlike the JRF/AβN/25 immunolabeling (Fig. 6), the majority of the APP detected by JRF/Aβtot/17 is not within early endosomes.

Whereas these results suggest a partial redistribution of APP to the cell surface following calpain inhibition, we further confirmed this finding by quantitative ^{125}I-mAb binding to intact and permeabilized cells (41). Table III shows the results of binding ^{125}I-JRF/Aβtot/17 to control L/APP cells as well as cells treated for 3 h with 10 μM calpeptin or calpain inhibitor III. Treatment with either inhibitor resulted in a small increase in the number of JRF/Aβtot/17 binding sites in permeabilized cells (~1.2-fold with both treatments), consistent with the slight increase in APP levels seen by Western blot analysis following calpain inhibition (Fig. 2). JRF/Aβtot/17 binding at the cell surface increased ~1.6-fold with inhibitor treatment, with the JRF/Aβtot/17 binding at the cell surface as a percentage of total binding increasing from 8.6 to ~11%. Thus, inhibiting calpains results in a partial redistribution of APP (and possibly βCTFs, since JRF/Aβtot/17 recognizes both species), so that the steady-state levels in the plasma membrane are increased. In an additional experiment, we did a similar analysis of surface *versus* total JRF/Aβtot/17 binding sites at multiple time points following the addition of 10 μM calpeptin (data not shown). We found that the increase in JRF/Aβtot/17 binding at the cell surface was extremely rapid (1.8-fold increase after 15-min treatment compared with a maximal 2.3-fold after 6 h). As previously seen, JRF/Aβtot/17 binding to permeabilized cells increased as well (remaining at 1.2-fold from 1.5 to 6 h), although the kinetics were somewhat slower than the increase in surface JRF/Aβtot/17 binding sites.

To determine the effect of calpain inhibition on βCTF levels and its cell surface distribution, we performed a similar quantitative ^{125}I-JRF/AβN/25 binding experiment (Table IV). Calpeptin and calpain inhibitor III increased the binding of JRF/AβN/25 to permeabilized cells by 2- and 2.5-fold, respectively, confirming the dramatic increase in the levels of this APP metabolite following calpain inhibition. Calpain inhibition also dramatically increased JRF/AβN/25 binding at the cell surface (nearly 5-fold). As a percentage of total JRF/AβN/25 binding, cell surface binding increased 2.8-fold with calpeptin treatment and 1.6-fold with calpain inhibitor III treatment. The roughly proportionate increase in total (average of 2.3-fold for both inhibitors) and cell surface (average 2.2-fold) JRF/AβN/25 binding suggests that βCTFs are in equilibrium between the intracellular pool and the plasma membrane population following calpain inhibition.

Taken together, these ^{125}I-mAb binding findings and the immunolabeling patterns seen in Figs. 5 and 6 indicate greater levels of APP holoprotein in the plasma membrane following calpain inhibition. Importantly, JRF/Aβtot/17 does not detect the αCTF, an important APP species seen with calpain inhibition (see Figs. 3 and 4) and an APP metabolite thought to be generated at the cell surface (7, 55). Therefore, the increase in JRF/Aβtot/17 binding to intact cells following calpain inhibition is likely to substantially underestimate the total pool of APP cell-associated metabolites (APP holoprotein, αCTF, and βCTF) found at the cell surface.

DISCUSSION

Our results confirm previous reports that calpain inhibition increases the secretion of Aβ42 relative to Aβ40 (36, 37, 39); in fact, we find that treating cells with calpain inhibitors increases Aβ42 production far beyond the increase due to the expression of FAD mutant PS1 in the same cell (Fig. 2) and beyond that generally reported by others following mutant PS1 expression in either cell culture or transgenic mice (16–18). A number of lines

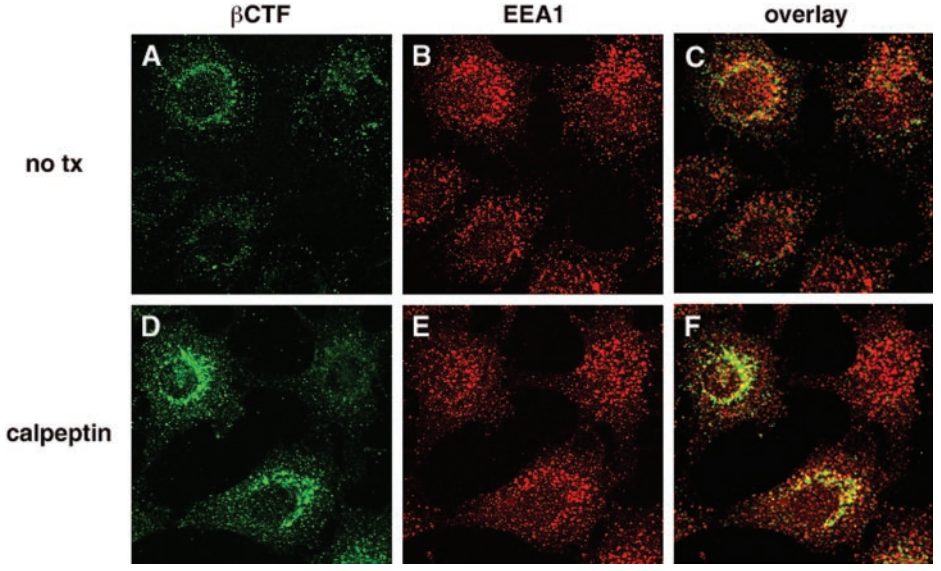

FIG. 6. **Intracellular localization of βCTFs.** L/APP cells were seeded onto glass coverslips, and APP expression was induced. Calpeptin at 10 μM was added for the final 6 h of incubation as indicated. *A* and *D*, indirect immunolabeling using JRF/AβN/25 and detected by confocal microscopy; *B* and *E*, immunolabeling with anti-EEA1 antiserum; *C* and *F*, overlay of the two immunolabeling patterns. Some cell-to-cell variability in the levels of human APP following butyrate induction is typical in these cells.

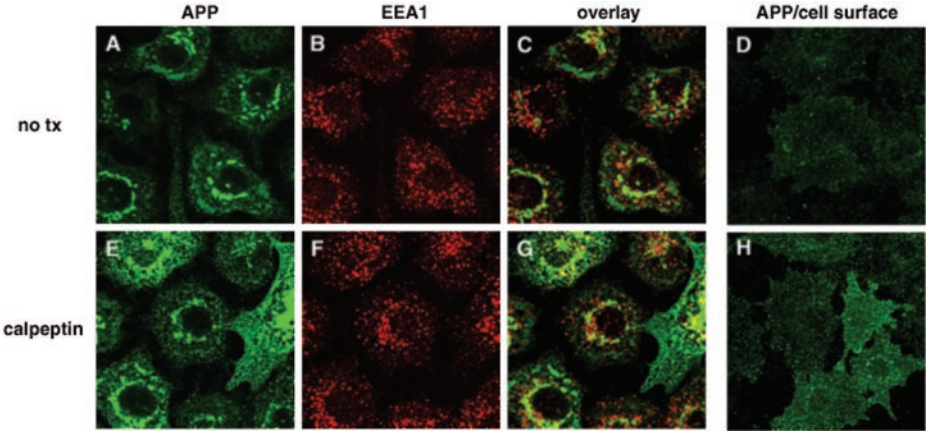

FIG. 7. **Cellular distribution of APP detected with JRF/Aβtot/17 following calpeptin treatment.** L/APP cells were grown, treated, and examined as in Fig. 6. *A*, *D*, *E*, and *H*, indirect immunolabeling with JRF/Aβtot/17; *B* and *F*, immunolabeling with anti-EEA1 antiserum; *C* and *G*, overlay of the two immunolabeling patterns. The cells shown in *A–C* and *E–G* were permeabilized prior to immunolabeling to show the complete distribution of APP within the cell. The cells in *D* and *H* were not permeabilized prior to immunolabeling to show the cell surface distribution of APP using JRF/Aβtot/17.

TABLE III
Calpain inhibition results in a partial redistribution of APP to the cell surface

Values are shown ± S.E.

	No treatment	10 μM calpeptin	10 μM calpain inhibitor III
		cpm	
Total JRF/Aβtot/17 binding	9219 ± 481	10,786 ± 339 ($p < 0.05$)	11,257 ± 239 ($p < 0.05$)
Surface JRF/Aβtot/17 binding	796 ± 29	1274 ± 88 ($p < 0.05$)	1236 ± 39 ($p < 0.001$)
Percentage of JRF/Aβtot/17 binding at cell surface	8.6 ± 0.3%	11.8 ± 0.8%	11.0 ± 0.3%

TABLE IV
Increased cell surface and intracellular βCTF levels following calpain inhibition

Values are shown ± S.E.

	No treatment	10 μM calpeptin	10 μM calpain inhibitor III
		cpm	
Total JRF/AβN/25 binding	983 ± 32	1928 ± 58 ($p < 0.001$)	2496 ± 60 ($p < 0.001$)
Surface JRF/AβN/25 binding	41 ± 3	225 ± 22 ($p < 0.01$)	174 ± 9 ($p < 0.01$)
Percentage of JRF/AβN/25 binding at cell surface	4.2 ± 0.2%	11.7 ± 1.2%	6.7 ± 0.4%

of evidence suggest that this effect results specifically from a reduction of calpain activity within the cell. In addition to the two inhibitors used in this study (calpeptin and calpain inhibitor III), others have shown similar effects using these and other calpain-selective peptidyl aldehyde protease inhibitors (38, 39). While many of these inhibitors can also inhibit the proteasome at high concentrations, Yamazaki *et al.* (36) demonstrated that the proteosome-selective inhibitor lactacystin did not increase Aβ42 secretion selectively, as did calpain-selective inhibitors. Additionally, in this study it was shown that cells treated with an inhibitory domain of calpastatin showed an increase in Aβ42 secretion relative to Aβ40, arguing for a direct role of calpain activity in this effect. Similarly, we have transiently overexpressed a single inhibitory domain of calpastatin in L/APP4 cells and seen increased APP immunolabeling at the cell surface in transfected cells.[2] The manipulation of calpain activity in a cell by calpastatin overexpression is likely to be the best mechanism

[2] S. D. Schmidt and P. M. Mathews, unpublished data.

to directly implicate calpain activity in APP trafficking and metabolism and is something we are currently pursuing.

Inhibiting Calpains Redistributes APP to the Cell Surface, Resulting in an Increase in α- and β-Cleavage—The distribution of APP between the TGN and the cell surface is highly regulated. Phosphorylation of APP by protein kinase C, for example, results in a redistribution of the protein to the plasma membrane, increasing α-cleavage while reducing Aβ generation (56, 57). Multiple lines of evidence suggest that much α-cleavage occurs at the cell surface, including shedding of cell surface iodinated APP as sAPPα (7), the localization of the proteolytically active form of ADAM 10 to the plasma membrane (5), and the significant reduction of α-cleavage by a cell-impermeant metalloproteinase inhibitor in a human neuroblastoma cell line (6). The picture may be more complex, however, since Lee and colleagues have proposed that the protein kinase C-regulated increase in α-cleavage occurs within the TGN, in contrast to constitutive α-cleavage, which occurs at the cell surface (58). Given that we detect a greater proportion of APP at the cell surface following calpain inhibition, the simplest explanation for the increase in α-cleavage seen in these cells would be the increased availability of APP for cell surface TACE and/or ADAM 10.

Moreover, the increase in both α- and β-cleavage is likely to be due to a rapid equilibrium between APP at the cell surface, where α-cleavage is likely to occur, and APP within early endosomes, where growing evidence points toward this compartment as being a major β-cleavage site. The evidence that cell surface APP is likely to be in rapid communication with early endosomes is substantial (59) and includes the findings that removal (14) or replacement (12) of the cytoplasmic tail of APP results in more APP at the cell surface by preventing its internalization. Koo and collaborators (13) have gone further by mapping discrete internalization motifs within this domain. Interestingly, those mutations that prevent or reduce the endocytosis of APP also reduce Aβ generation, one line of evidence that endosomes are critical sites for either β- or γ-cleavage. Most reports have now placed BACE within early endosomes and/or throughout the endosomal-lysosomal system (9–11), although some disagreement remains as to other intracellular compartments where this protease might be located (60). Coupled with our data showing βCTFs within early endosomes (Fig. 5), this strongly suggests that early endosomes are a major, if not the major, site for β-cleavage of APP.

Our findings support a model in which the intracellular distribution of APP is altered by calpain inhibition. Our data directly support increased levels of APP at the cell surface following calpain inhibition, and rapid communication between the plasma membrane and early endosome is likely (14). Were these two compartments in equilibrium, such an increase in APP levels would result in a similar increase in both α-cleavage at the cell surface and β-cleavage within early endosomes, as we found by metabolic labeling and immunoprecipitation. This redistribution of APP toward the plasma membrane/early endosome from the TGN could result from either of two, not mutually exclusive, mechanisms: 1) APP egress from the TGN is increased and/or 2) recycling of APP from the cell surface/early endosome to the TGN is inhibited. Such a TGN recycling pathway plays a critical role in maintaining the distribution of some proteins that are primarily found within the TGN but also at the cell surface (*e.g.* furin (61) and TGN38 (62)). Additional experimentation will be required to determine whether the TGN recycling pathway contributes to the subcellular distribution of APP. Nevertheless, if this were the case, it would raise the possibility that other metabolites of APP, such as the βCTF, may also recycle, permitting APP fragments generated in early endosomes to return to the Golgi apparatus, perhaps to undergo further proteolytic processing (*e.g.* γ-cleavage).

Relationship of Calpain Inhibition and γ-42-Secretase Activity—Whereas the changes in the intracellular distribution of APP following calpain inhibition appear to lead to increased βCTF production and then to drive Aβ42 generation, we do not yet know why these additional βCTFs are substrates primarily for γ-42-secretase activity. One possibility is that inhibiting calpains has a direct impact on the γ-secretase activity of a cell, favoring γ-42-secretase activity over γ-40-secretase activity. The available evidence suggests that this is, at best, only a partial explanation of the calpain inhibition effect. We and others (36, 37, 39) have shown that Aβ40 production remains the same or is slightly increased following calpain inhibition, suggesting that calpain inhibition does not prevent γ-40-secretase activity, thereby driving all γ-cleavage toward a γ-42-secretase pathway. Additionally, we were unable to saturate Aβ42 production with increasing concentrations of calpain inhibitors in either control or mutant PS1-expressing L cells. Whereas these experiments are limited by the toxicity of these inhibitors at the highest concentration, the increase in Aβ42 appeared to closely parallel the increase in CTFs. This suggests two distinct mechanisms by which Aβ42 production can be increased: by modified activity of the presenilin complex independent of an increase in βCTFs (*e.g.* mutant PS (16–18)) or in a βCTF-dependent fashion following calpain inhibition. Interestingly, an interaction between the large cytoplasmic loop domain of PS2 and μ-calpain has been reported, suggesting that calpains may directly regulate PS function (63), potentially linking calpain activity with γ-secretase function. A second possibility is that the subcellular compartment in which γ-cleavage occurs can play a critical role in determining whether Aβ40 or Aβ42 is generated (64). Some experiments have shown early endosomes to have the capacity to generate Aβ42 (13), with others suggesting that compartments within the secretory pathway may (65) or may not (66) generate Aβ42. If calpain inhibition affects the intracellular trafficking of the βCTF as well as APP, it may well be that the βCTFs are directed to a compartment(s) within the cell that is primarily γ42-cleavage-competent.

Relationship between the Calpain System and Neurodegeneration—Generally, increased calpain activity is thought to play a role in the development of pathological cytoskeletal changes (32–35) or to place a neuron at greater risk following an additional insult. At higher levels of activation, calpains may directly precipitate cell death, particularly in ischemia and excitotoxicity (28, 29). If reduced calpain activity were to promote AD pathology by increasing Aβ generation, particularly Aβ42, this would contrast with increased calpain activity promoting pathological tau changes. It may be that during the extended time course of AD in humans, the calpain system plays multiple roles, initially promoting Aβ generation and, later in the disease, responding to and exacerbating tau pathology. Both a greater understanding of the role of the calpain system in APP metabolism and a better assessment of endogenous calpain activity in neurons (67) will be necessary to dissect the relationship between either decreased or increased calpain activity and developing pathology. Nevertheless, as our understanding of the complex relationships between calpain activity and the regulation of seemingly disparate cellular events grows, the probability that calpains are intimately involved in the disease process appears likely. Finally, this study and previous studies (36, 37, 39) should raise concern as calpain inhibitors are aggressively pursued for their neuroprotective effects. Chronically inhibiting calpain activity and, there-

fore, inducing a dramatic increase in Aβ42 generation may have negative consequences.

Acknowledgments—We thank Stephen P. Jacobsen for help with figures and Dr. Suzana Petanceska for helpful discussions. We also thank Dr. Silvia Corvera (University of Massachusetts Medical School, Worcester, MA) for the kind gift of the anti-EEA1 antibody and Nicole Terrio in our group for antibody production.

REFERENCES

1. De Strooper, B., and Annaert, W. (2000) *J. Cell Sci.* **113,** 1857–1870
2. Buxbaum, J. D., Liu, K. N., Luo, Y., Slack, J. L., Stocking, K. L., Peschon, J. J., Johnson, R. S., Castner, B. J., Cerretti, D. P., and Black, R. A. (1998) *J. Biol. Chem.* **273,** 27765–27767
3. Slack, B. E., Ma, L. K., and Seah, C. C. (2001) *Biochem. J.* **357,** 787–794
4. Lopez-Perez, E., Zhang, Y., Frank, S. J., Creemers, J., Seidah, N., and Checler, F. (2001) *J. Neurochem.* **76,** 1532–1539
5. Lammich, S., Kojro, E., Postina, R., Gilbert, S., Pfeiffer, R., Jasionowski, M., Haass, C., and Fahrenholz, F. (1999) *Proc. Natl. Acad. Sci. U. S. A.* **96,** 3922–3927
6. Parvathy, S., Hussain, I., Karran, E. H., Turner, A. J., and Hooper, N. M. (1999) *Biochemistry* **38,** 9728–9734
7. Sisodia, S. S. (1992) *Proc. Natl. Acad. Sci. U. S. A.* **89,** 6075–6079
8. Lin, X., Koelsch, G., Wu, S., Downs, D., Dashti, A., and Tang, J. (2000) *Proc. Natl. Acad. Sci. U. S. A.* **97,** 1456–1460
9. Vassar, R., Bennett, B. D., Babu-Khan, S., Kahn, S., Mendiaz, E. A., Denis, P., Teplow, D. B., Ross, S., Amarante, P., Loeloff, R., Luo, Y., Fisher, S., Fuller, J., Edenson, S., Lile, J., Jarosinski, M. A., Biere, A. L., Curran, E., Burgess, T., Louis, J. C., Collins, F., Treanor, J., Rogers, G., and Citron, M. (1999) *Science* **286,** 735–741
10. Capell, A., Steiner, H., Willem, M., Kaiser, H., Meyer, C., Walter, J., Lammich, S., Multhaup, G., and Haass, C. (2000) *J. Biol. Chem.* **275,** 30849–30854
11. Walter, J., Fluhrer, R., Hartung, B., Willem, M., Kaether, C., Capell, A., Lammich, S., Multhaup, G., and Haass, C. (2001) *J. Biol. Chem.* **276,** 14634–14641
12. Soriano, S., Chyung, A. S., Chen, X., Stokin, G. B., Lee, V. M., and Koo, E. H. (1999) *J. Biol. Chem.* **274,** 32295–32300
13. Perez, R. G., Soriano, S., Hayes, J. D., Ostaszewski, B., Xia, W., Selkoe, D. J., Chen, X., Stokin, G. B., and Koo, E. H. (1999) *J. Biol. Chem.* **274,** 18851–18856
14. Koo, E. H., and Squazzo, S. L. (1994) *J. Biol. Chem.* **269,** 17386–17389
15. Cataldo, A. M., Peterhoff, C. M., Troncoso, J. C., Gomez-Isla, T., Hyman, B. T., and Nixon, R. A. (2000) *Am. J. Pathol.* **157,** 277–286
16. Duff, K., Eckman, C., Zehr, C., Yu, X., Prada, C. M., Perez-tur, J., Hutton, M., Buee, L., Harigaya, Y., Yager, D., Morgan, D., Gordon, M. N., Holcomb, L., Refolo, L., Zenk, B., Hardy, J., and Younkin, S. (1996) *Nature* **383,** 710–713
17. Borchelt, D. R., Thinakaran, G., Eckman, C. B., Lee, M. K., Davenport, F., Ratovitsky, T., Prada, C. M., Kim, G., Seekins, S., Yager, D., Slunt, H. H., Wang, R., Seeger, M., Levey, A. I., Gandy, S. E., Copeland, N. G., Jenkins, N. A., Price, D. L., Younkin, S. G., and Sisodia, S. S. (1996) *Neuron* **17,** 1005–1013
18. Citron, M., Westaway, D., Xia, W., Carlson, G., Diehl, T., Levesque, G., Johnson-Wood, K., Lee, M., Seubert, P., Davis, A., Kholodenko, D., Motter, R., Sherrington, R., Perry, B., Yao, H., Strome, R., Lieberburg, I., Rommens, J., Kim, S., Schenk, D., Fraser, P., St. George Hyslop, P., and Selkoe, D. J. (1997) *Nat. Med.* **3,** 67–72
19. Shen, J., Bronson, R. T., Chen, D. F., Xia, W., Selkoe, D. J., and Tonegawa, S. (1997) *Cell* **89,** 629–639
20. De Strooper, B., Saftig, P., Craessaerts, K., Vanderstichele, H., Guhde, G., Annaert, W., Von Figura, K., and Van Leuven, F. (1998) *Nature* **391,** 387–390
21. Wolfe, M. S., Xia, W., Ostaszewski, B. L., Diehl, T. S., Kimberly, W. T., and Selkoe, D. J. (1999) *Nature* **398,** 513–517
22. Yu, G., Nishimura, M., Arawaka, S., Levitan, D., Zhang, L., Tandon, A., Song, Y. Q., Rogaeva, E., Chen, F., Kawarai, T., Supala, A., Levesque, L., Yu, H., Yang, D. S., Holmes, E., Milman, P., Liang, Y., Zhang, D. M., Xu, D. H., Sato, C., Rogaev, E., Smith, M., Janus, C., Zhang, Y., Aebersold, R., Farrer, L. S., Sorbi, S., Bruni, A., Fraser, P., and St. George-Hyslop, P. (2000) *Nature* **407,** 48–54
23. Sorimachi, H., Ishiura, S., and Suzuki, K. (1997) *Biochem. J.* **328,** 721–732
24. Croall, D. E., and DeMartino, G. N. (1991) *Physiol. Rev.* **71,** 813–847
25. Maki, M., Ma, H., Takano, E., Adachi, Y., Lee, W. J., Hatanaka, M., and Murachi, T. (1991) *Biomed. Biochim. Acta* **50,** 509–516
26. Nixon, R. A., Saito, K. I., Grynspan, F., Griffin, W. R., Katayama, S., Honda, T., Mohan, P. S., Shea, T. B., and Beermann, M. (1994) *Ann. N. Y. Acad. Sci.* **747,** 77–91
27. Sato, K., Saito, Y., and Kawashima, S. (1995) *Eur. J. Biochem.* **230,** 25–31
28. Bartus, R. T., Elliott, P. J., Hayward, N. J., Dean, R. L., Harbeson, S., Straub, J. A., Li, Z., and Powers, J. C. (1995) *Neurol. Res.* **17,** 249–258
29. Wang, K. K. (2000) *Trends Neurosci.* **23,** 20–26
30. Saito, K., Elce, J. S., Hamos, J. E., and Nixon, R. A. (1993) *Proc. Natl. Acad. Sci. U. S. A.* **90,** 2628–2632
31. Grynspan, F., Griffin, W. R., Cataldo, A., Katayama, S., and Nixon, R. A. (1997) *Brain Res.* **763,** 145–158
32. Lee, M. S., Kwon, Y. T., Li, M., Peng, J., Friedlander, R. M., and Tsai, L. H. (2000) *Nature* **405,** 360–364
33. Shea, T. B., Spencer, M. J., Beermann, M. L., Cressman, C. M., and Nixon, R. A. (1996) *J. Neurochem.* **66,** 1539–1549
34. Xie, H., and Johnson, G. V. (1997) *J. Neurochem.* **69,** 1020–1030
35. Xie, H. Q., and Johnson, G. V. (1998) *J. Neurosci. Res.* **53,** 153–164
36. Yamazaki, T., Haass, C., Saido, T. C., Omura, S., and Ihara, Y. (1997) *Biochemistry* **36,** 8377–8383
37. Yamazaki, T., and Ihara, Y. (1998) *Neurobiol. Aging* **19,** S77–S79
38. Klafki, H., Abramowski, D., Swoboda, R., Paganetti, P. A., and Staufenbiel, M. (1996) *J. Biol. Chem.* **271,** 28655–28659
39. Zhang, L., Song, L., and Parker, E. M. (1999) *J. Biol. Chem.* **274,** 8966–8972
40. Verdile, G., Martins, R. N., Duthie, M., Holmes, E., St. George-Hyslop, P. H., and Fraser, P. E. (2000) *J. Biol. Chem.* **275,** 20794–20798
41. Mathews, P. M., Martinie, J. B., and Fambrough, D. M. (1992) *J. Cell Biol.* **118,** 1027–1040
42. Mathews, P. M., Guerra, C. B., Jiang, Y., Grbovic, O. M., Kao, B. H., Schmidt, S. D., Dinakar, R., Mercken, M., Hille-Rehfeld, A., Rohrer, J., Mehta, P., Cataldo, A. M., and Nixon, R. A. (2002) *J. Biol. Chem.* **277,** 5299–5307
43. Wisniewski, T., Dowjat, W. K., Buxbaum, J. D., Khorkova, O., Efthimiopoulos, S., Kulczycki, J., Lojkowska, W., Wegiel, J., Wisniewski, H. M., and Frangione, B. (1998) *Neuroreport* **9,** 217–221
44. Mathews, P. M., Cataldo, A. M., Kao, B. H., Rudnicki, A. G., Qin, X., Yang, J. L., Jiang, Y., Picciano, M., Hulette, C., Lippa, C. F., Bird, T. D., Nochlin, D., Walter, J., Haass, C., Levesque, L., Fraser, P. E., Andreadis, A., and Nixon, R. A. (2000) *Mol. Med.* **6,** 878–891
45. Neill, D., Hughes, D., Edwardson, J. A., Rima, B. K., and Allsop, D. (1994) *J. Neurosci. Res.* **39,** 482–493
46. Vandermeeren, M., Geraerts, M., Pype, S., Dillen, L., Van Hove, C., and Mercken, M. (2001) *Neurosci. Lett.* **315,** 145–148
47. Janus, C., Pearson, J., McLaurin, J., Mathews, P. M., Jiang, Y., Schmidt, S. D., Chishti, M. A., Horne, P., Heslin, D., French, J., Mount, H. T., Nixon, R. A., Mercken, M., Bergeron, C., Fraser, P. E., St. George-Hyslop, P., and Westaway, D. (2000) *Nature* **408,** 979–982
48. Van Nostrand, W. E., Wagner, S. L., Suzuki, M., Choi, B. H., Farrow, J. S., Geddes, J. W., Cotman, C. W., and Cunningham, D. D. (1989) *Nature* **341,** 546–549
49. Patki, V., Virbasius, J., Lane, W. S., Toh, B. H., Shpetner, H. S., and Corvera, S. (1997) *Proc. Natl. Acad. Sci. U. S. A.* **94,** 7326–7330
50. Lawe, D. C., Patki, V., Heller-Harrison, R., Lambright, D., and Corvera, S. (2000) *J. Biol. Chem.* **275,** 3699–3705
51. Rozmahel, R., Huang, J., Chen, F., Liang, Y., Nguyen, V., Ikeda, M., Levesque, G., Yu, G., Nishimura, M., Mathews, P., Schmidt, S. D., Mercken, M., Bergeron, C., Westaway, D., and St. George-Hyslop, P. (2002) *Neurobiol. Aging* **23,** 187–194
52. Beggah, A., Mathews, P., Beguin, P., and Geering, K. (1996) *J. Biol. Chem.* **271,** 20895–20902
53. Gaullier, J. M., Ronning, E., Gillooly, D. J., and Stenmark, H. (2000) *J. Biol. Chem.* **275,** 24595–24600
54. Mu, F. T., Callaghan, J. M., Steele-Mortimer, O., Stenmark, H., Parton, R. G., Campbell, P. L., McCluskey, J., Yeo, J. P., Tock, E. P., and Toh, B. H. (1995) *J. Biol. Chem.* **270,** 13503–13511
55. Maruyama, K., Kametani, F., Usami, M., Yamao-Harigaya, W., and Tanaka, K. (1991) *Biochem. Biophys. Res. Commun.* **179,** 1670–1676
56. Gandy, S., Caporaso, G., Buxbaum, J., Frangione, B., and Greengard, P. (1994) *Neurobiol. Aging* **15,** 253–256
57. Caporaso, G. L., Gandy, S. E., Buxbaum, J. D., Ramabhadran, T. V., and Greengard, P. (1992) *Proc. Natl. Acad. Sci. U. S. A.* **89,** 3055–3059
58. Skovronsky, D. M., Moore, D. B., Milla, M. E., Doms, R. W., and Lee, V. M. (2000) *J. Biol. Chem.* **275,** 2568–2575
59. Selkoe, D. J., Yamazaki, T., Citron, M., Podlisny, M. B., Koo, E. H., Teplow, D. B., and Haass, C. (1996) *Ann. N. Y. Acad. Sci.* **777,** 57–64
60. Yan, R., Han, P., Miao, H., Greengard, P., and Xu, H. (2001) *J. Biol. Chem.* **276,** 36788–36796
61. Mallet, W. G., and Maxfield, F. R. (1999) *J. Cell Biol.* **146,** 345–359
62. Ghosh, R. N., Mallet, W. G., Soe, T. T., McGraw, T. E., and Maxfield, F. R. (1998) *J. Cell Biol.* **142,** 923–936
63. Shinozaki, K., Maruyama, K., Kume, H., Tomita, T., Saido, T. C., Iwatsubo, T., and Obata, K. (1998) *Int. J. Mol. Med.* **1,** 797–799
64. Greenfield, J. P., Tsai, J., Gouras, G. K., Hai, B., Thinakaran, G., Checler, F., Sisodia, S. S., Greengard, P., and Xu, H. (1999) *Proc. Natl. Acad. Sci. U. S. A.* **96,** 742–747
65. Cook, D. G., Forman, M. S., Sung, J. C., Leight, S., Kolson, D. L., Iwatsubo, T., Lee, V. M., and Doms, R. W. (1997) *Nat. Med.* **3,** 1021–1023
66. Maltese, W. A., Wilson, S., Tan, Y., Suomensaari, S., Sinha, S., Barbour, R., and McConlogue, L. (2001) *J. Biol. Chem.* **276,** 20267–20279
67. Taniguchi, S., Fujita, Y., Hayashi, S., Kakita, A., Takahashi, H., Murayama, S., Saido, T. C., Hisanaga, S., Iwatsubo, T., and Hasegawa, M. (2001) *FEBS Lett.* **489,** 46–50